Journal of Nuclear Medicine, published on February 22, 2019 as doi:10.2967/jnumed.118.222638

Enhancement of astatine-211 uptake via the sodium iodide symporter by the addition of ascorbic acid in targeted alpha therapy of thyroid cancer

Tadashi Watabe[1], Kazuko Kaneda-Nakashima[2], Yuwei Liu[1], Yoshifumi Shirakami[1], Kazuhiro Ooe[1], Atsushi Toyoshima[3], Eku Shimosegawa[4], Mitsuhiro Fukuda[5], Atsushi Shinohara[6], Jun Hatazawa[1]

[1] Department of Nuclear Medicine and Tracer Kinetics, Osaka University Graduate School of Medicine

[2] Core for Medicine and Science Collaborative Research and Education, Project Research

Center for Fundamental Sciences, Osaka University Graduate School of Science

[3] Institute for Radiation Sciences, Osaka University

[4] Department of Molecular Imaging in Medicine, Osaka University Graduate School of Medicine

[5] Research Center for Nuclear Physics, Osaka University

[6] Department of Chemistry, Graduate School of Science, Osaka University, Toyonaka Osaka Japan

Corresponding and first author:

Tadashi Watabe (Assistant Professor)

2-2 Yamadaoka, Suita, Osaka 565-0871 JAPAN

TEL: +81-6-6879-3461 FAX: +81-6-6879-3469

E-Mail: watabe@tracer.med.osaka-u.ac.jp

Total word count: 4,999 words

Short running title: Astatine-211 for thyroid cancer

ABSTRACT

^{211}At is an alpha-emitter which has similar chemical properties to iodine and is used in targeted alpha therapy. In the present study, we added ascorbic acid (AA) to ^{211}At solution to increase the radiochemical purity of astatide and evaluated its efficacy against differentiated thyroid cancer, which is characterized by the expression of sodium/iodide symporter (NIS).

Methods: Crude ^{211}At solution (AA(-) solution) and ^{211}At solution treated with AA (AA(+) solution) were prepared. Uptakes by the thyroid were compared between the two solutions in normal male Wistar rats (n = 6). Cellular uptake analysis in K1-NIS cells was performed under the AA(+) and AA(-) conditions. AA(+) solution was injected at three doses into K1-NIS xenograft mice: 1 MBq (n = 6), 0.4 MBq (n = 6), and 0.1 MBq (n = 6), and vehicle was injected into control mice (n = 6). The treatment effects were compared among the four groups.

Results: Uptake by the thyroid was significantly enhanced in rats injected with the AA(+) solution as compared to those injected with AA(-) solution. Cellular uptake analysis showed significantly increased uptake of ^{211}At by the K1-NIS cells under the AA(+) condition as compared to the AA(-) condition. In the mouse xenograft model, the K1-NIS tumors showed significant accumulation of ^{211}At at 3 and 24 hr post administration (22.5 ± 10.4% ID and 12.9 ± 6.8% ID, respectively). Tumor growth was immediately inhibited in a dose-dependent manner after administration of ^{211}At. In the survival analysis, the ^{211}At groups (0.1, 0.4, and 1 MBq) showed significantly better survival than the control group.

Conclusion: Uptake of ^{211}At was enhanced in differentiated thyroid cancer cells as well as the normal thyroid using ^{211}At solution treated with AA. It also showed dose-dependent efficacy against the K1-NIS xenografts, suggesting its potential applicability to targeted alpha therapy.

Keywords astatine; thyroid cancer; sodium iodide symporter; alpha therapy; ascorbic acid

INTRODUCTION

Radioactive iodine has long been used clinically for patients with differentiated thyroid cancer (*1-3*). ^{131}I is used for the ablation of thyroid remnants or treatment of metastatic thyroid cancer (*1*). However, some patients with multiple metastases are refractory to repetitive ^{131}I treatment, despite the targeted regions showing sufficient iodine uptake (*4,5*). According to the criteria described in the 2015 American Thyroid Association guidelines, radioactive iodine-refractory cancer includes metastatic disease that progresses despite showing substantial uptake of radioactive iodine (*6*). In such patients, beta-particle therapy using ^{131}I is inadequate and another strategy is needed using more effective radionuclide targeting the sodium/iodide symporter (NIS).

Astatine (^{211}At) is receiving increasing attention as an alpha-emitter for targeted radionuclide therapy (*7-9*). ^{211}At is a halogen element with similar chemical properties to iodine (*10*). Alpha particles emitted from ^{211}At with a branching ratio

of 41.8% (5.98MeV) has higher linear energy transfer as compared to beta particles from ^{131}I (0.97MeV) and exert a better therapeutic effect by inducing DNA double strand breaks and free radical formation (*11*). Petrich et al. reported that ^{211}At accumulated in the normal thyroid and in tumor xenografts of a genetically modified NIS-expressing papillary thyroid cancer cell line (*12*). They also showed that ^{211}At was effective against thyroid cancer xenografts (*12*). Meanwhile, the oxidative states of ^{211}At solutions may vary and the chemical form and dynamics in the body of ^{211}At have not yet been clearly elucidated, because there is no stable isotope of ^{211}At (*13,14*). It is presumed that a plenty of astatine species such as At^+, AtO^-, $At(OH)_2^-$, AtO_2^-, $AtO(OH)_2^-$ and AtO^+ as well as At^- are presented in a basic or acidic aqueous solutions under a oxidative or reductive condition. In many radiopharmaceutical solutions, ascorbic acid (AA) is frequently added as stabilizing agent since it is a vitamin C and can be safely administered in humans. There is a possibility of stabilizing the oxidative states of ^{211}At in its solutions by adding

appropriate reducing agent. In the present study, we prepared ^{211}At solutions focusing on the radiochemical purity of astatide (or astatide ion) and evaluated its distribution in the normal thyroid tissue via transport through NIS, as well as its efficacy against differentiated thyroid cancer in a tumor xenograft model.

MATERIALS AND METHODS

Preparation of the ^{211}At Solutions

^{211}At was produced by the ^{209}Bi(α, 2n)^{211}At reaction, followed by the separation and purification by a dry distillation method. ^{211}At was dissolved in 100 μL of distilled water. The ^{211}At-crude solution at a final concentration of 10 MBq/mL was mixed with AA as a reducing agent at a final concentration of 1.2 w/v% and sodium bicarbonate as a pH adjuster at a final concentration of 2.1 w/v% at pH8.0, and allowed to stand for 1 hour at ambient temperature. Separately, the ^{211}At-crude solution was also mixed with the other reducing agents, namely, cysteine,

glutathione, sodium sulfite or ferrous sulfate, at a final concentration of 1 w/v% under the same conditions. The resultant mixtures of ^{211}At solutions were analyzed by thin-layer chromatography using Typhoon 7000 (GE Healthcare). The reagents were purchased from Nacalai Tesque (Kyoto, Japan).

***In vitro* Cellular Uptake and Survival Analysis**

K1 cells (human papillary thyroid carcinoma) was provided by the European Collection of Authenticated Cell Cultures. K1 cells were maintained in culture medium, D-MEM:Ham's F12:MCDB 105 (2:1:1) supplemented with 2 mM Glutamine and 10% heat-inactivated fatal bovine serum (FBS). K1-NIS cells were obtained by the transfection using the human SLC5A5 (NIS) gene clone (OriGene). K1 cells and K1-NIS cells were seeded onto a 24-well plate (1×10^5/well) and cultured for 2 days. After treatment of ^{211}At, the cells were washed twice with PBS(-) and the radioactivity was measured using a 2480 Wizard^2 gamma counter (Perkin Elmer).

K1-NIS cells were seeded onto a 96-well plate (2×10^4/well) and cultured for 2 days. ^{211}At and ^{131}I were serially diluted with the culture medium (100μL/well). After 48hr of incubation, we measured cell viability using Cell counting-kit 8 (Dojindo).

Preparation of Animals

Normal male Wistar rats and male ICR and SCID mice were purchased from Japan SLC Inc. (Hamamatsu, Japan) and Charles River Japan, Inc. (Atsugi, Japan), respectively. Animals were housed under a 12-h light/12-h dark cycle, and given free access to food and water. The Wistar rats were fed with a low-iodine diet two weeks before the experiment to make the thyroid condition uniform, in accordance with the method used in a previous study (*15*). Tumor xenograft models were established by subcutaneous injection of K1-NIS cells (1-2 × 10^7 cells) suspended in 0.2 mL of culture medium and Matrigel (1:1; BD Biosciences) into the SCID mice.

All the animal experiments were performed in compliance with the guidelines of the Institute of Experimental Animal Sciences. The protocol was approved by the Animal Care and Use Committee of the Osaka University Graduate School of Medicine. The criteria for euthanasia were as follows: 1) when the animals have intolerable suffering, 2) when a significant decrease in activity or a marked decrease in food and water intake was observed, and 3) end of the observation period (up to 84 days). The euthanasia was performed by deep anesthesia by isoflurane inhalation.

Administration of the ^{211}At Solutions and Imaging Analysis

Two groups of normal Wistar rats (n = 6; 12 weeks old; body weight = 295.2 ± 16.2 g) were anesthetized with 2% isoflurane and injected with the ^{211}At solutions (AA(-) ^{211}At solution (3.58 ± 0.65 MBq) or AA(+) ^{211}At solution (2.72 ± 0.12 MBq)) through the tail vein. Normal ICR mice (n = 11; 10 weeks old; body weight

= 37.9 ± 1.6 g) were used for the evaluation of toxicity at 3, 7 and 15 days after administration of AA(+) ^{211}At solution (1.00 ± 0.16 MBq).

K1-NIS tumor xenograft mice (n = 24; 10 weeks old; body weight = 21.4 ± 1.92 g) were investigated 37 days, on average, after implantation, when the tumor size reached approximately 10 mm in diameter. Under 2% isoflurane anesthesia, K1-NIS mice were injected with AA(+) ^{211}At solution through the tail vein. Mice were divided into 4 groups according to the injected dose (1 MBq (n = 6, 0.99 ± 0.09 MBq), 0.4 MBq (n = 6, 0.39 ± 0.13 MBq) 0.1 MBq (n = 6, 0.11 ± 0.07 MBq) and control (n = 6) groups). In the control group, vehicle solution and AA were administered.

Planar and SPECT images were acquired with a gamma camera system (E-cam, Siemens) with a low-energy all purpose collimator (*16*). The energy window was set at 79 keV ± 20% targeting the X-rays emitted from the daughter nuclide of ^{211}Po (*17*). The radioactivity in the major organs were measured with a gamma counter after

euthanasia and dissection at 24 hr. Regions of interest were placed using the AMIDE software (Ver. 1.0.4). Radioactivity levels in the major organs were measured with a gamma counter after euthanasia and dissection at 24 hr. Uptakes were normalized by the injected dose (MBq) and body weight (g). The equivalent dose (Gy) in the dosimetry of ^{211}At was estimated according to a previous report (*18*). Tumoral uptakes were estimated from the planar images at 3 and 24 hr post injection, and the area under the curve after 24 hr was assumed to decrease with physical decay.

Histological Analysis

After the animals were sacrificed by euthanasia, the tumor, thyroid and stomach were resected. The specimens were fixed overnight with 4% paraformaldehyde and cryoprotected in 30% sucrose in PBS. Frozen sections of the samples were then incubated with NIS-antibody (Anti-SLC5A5, Rabbit-Poly, Atlas antibodies). Immunohistochemistry was performed using the Dako EnVision + system - HRP

Labelled Polymer Anti-Rabbit (K4003) (DAKO Corp.). For the evaluation of toxicity, the thyroid and stomach were resected and frozen sections were stained with hematoxylin and eosin (H&E).

Statistical Analysis

Comparisons of the values between two groups were carried out using an unpaired t-test. Statistical analyses were carried out using SPSS (version 19.0) and probability values of less than 0.05 were considered to denote statistical significance. Survival analysis was performed using the Kaplan-Meier method, and the log-rank test with Holm correction was used for the group comparison.

RESULTS

TLC analysis depicted that the crude ^{211}At solution was a mixture of at least 3 chemical species of ^{211}At, as shown in Figure 1a. While the AA(+) ^{211}At solution was composed of a single chemical species of ^{211}At (Rf 0.79) with a

high radiochemical yield (95.7%), this species showed a similar TLC profile to that of ^{123}I-NaI (I^-, Rf 0.85). Figure 1b shows the TLC profiles of the ^{211}At solutions after addition of various reducing agents. Cysteine and glutathione also provided high radiochemical purity of the ^{211}At-asatide ions, but less than that noted under the AA(+) condition. On the other hand, sodium sulfite and ferrous sulfate, had no significant effect on the TLC profiles of the crude ^{211}At solutions under these conditions. Among the various reducing agents, addition of AA provided the highest radiochemical purity of the ^{211}At solution and it was stable for 24 hours. We used AA as the reducing agent for further experiments.

Whole-body distributions of ^{211}At in the normal rats are shown in Figure 2. High uptakes were observed in the thyroid, stomach and bladder in both planar and SPECT images. Uptake by the thyroid was significantly enhanced following administration of the AA(+) solution as compared to that following administration of the AA(-) solution. Measurement using the gamma counter

also showed high accumulation and significantly enhanced thyroid uptake following injection of the AA(+) solution as compared to the AA(-) solution (Table 1).

Cellular uptake analysis showed high uptake of ^{211}At in the K1-NIS cells, but almost no uptake in the K1 cells (Fig. 3a), suggesting that ^{211}At is transported into differentiated thyroid cancer cells through NIS. Uptake in the K1-NIS cells was significantly increased under the AA(+) condition as compared to the AA(-) condition (Fig. 3b).

The mouse tumor xenograft model revealed high accumulation in the K1-NIS tumor at 3 and 24 hr post administration (Fig. 4a). Planar images revealed that the activity concentration of ^{211}At was 22.5 ± 10.4% ID at 3 hr and 12.9 ± 6.8% ID at 24 hr in the K1-NIS xenograft. The equivalent dose in the tumor was estimated to be 9.7 ± 7.0 Gy. Measurement of the radioactivity in the K1-NIS xenografts (n = 3) at 24 hr after the injection of ^{211}At was shown in Table 2.

The change in the tumor size after administration of ^{211}At is shown in Figure 5a. Tumor growth was inhibited immediately after administration of ^{211}At and the treatment effect was dose-dependent. In the 1 MBq group, the tumor growth was suppressed until approximately 40 days after the injection and regrowth was relatively slow. In regard to the body weight, there was a slight drop in the 1 MBq group as compared to the other groups (Fig. 5b). However, this effect was transient, with the body weight restored within two weeks and remaining relatively stable thereafter. For the survival analysis, the ^{211}At administration groups (0.1, 0.4, and 1 MBq) showed significantly better survival rates as compared to the control group (Fig. 5c).

Expression of NIS was confirmed in the K1-NIS tumor xenografts, thyroid and stomach wall by immunohistochemical staining (Fig. 6).

DISCUSSION

In the present study, we demonstrated that the radiochemical purity of ^{211}At was increased by treatment with ascorbic acid. Uptake of ascorbic acid-treated ^{211}At was enhanced in the NIS-expressing cells in in-vitro studies, and in the normal thyroid after intravenous administration.

The AA(+) solution showed a dose-dependent treatment effect in the K1-NIS xenograft models. The ^{211}At is a very promising alpha-emitter as it can be produced in an accelerator and has similar chemical properties to iodine (*10*). However, one of the major problems of astatine is that there is no stable isotope and the basic chemistry is poorly understood (*18*). In previous publications of ^{211}At, the oxidation states of aqueous solutions of astatine, such as At^-, At(0), HOAt, AtO_3^-, H_5AtO_6, vary (*19*). In the present study, we found that the oxidation states of ^{211}At converged into one component, which is assumed to be astatide ion (At^-) according to the TLC analysis using ^{123}I and ^{211}At. ^{211}At-astatide ions are labile in aqueous solutions and

easily oxidized to higher oxidation states (*18-20*). Several reducing agents, including AA, were useful for the preparation of ^{211}At-astatide ions in aqueous solution as well as for the stabilization. TLC analyses of the solutions are desired, since the quality of the solutions vary.

In a previous study, in which the distribution of astatine was evaluated, high uptakes were observed in the thyroid, stomach, lungs, and spleen (*10,18*). Astatine is actively transported across the plasma membrane into the cytoplasm via NIS (*12*). The thyroid and stomach also showed high accumulation of iodine, reflecting the expression of NIS (*18*). These results were compatible with the whole-body distribution in the normal rats of our study, suggesting NIS is the key symporter in the uptake process of astatine.

As shown in Figure 6, stomach cells also showed NIS expression. However, no significant increase of ^{211}At uptake was observed in the stomach following administration of AA(+) solution as compared to the AA(-) solution. Spetz et al.

reported the difference in the whole-body distribution between ^{211}At and ^{125}I/^{131}I (*18*). In their study, less uptake of ^{211}At by the thyroid and higher uptake in the stomach were observed as compared to ^{125}I/^{131}I. Their study suggested that the transport mechanism of ^{211}At via NIS might be different between the thyroid and the stomach. There are some differences in the NIS expression by glycosylation modification, dimerization, and transcriptional regulation (including epigenetic regulation) (*21*). It is possible that these factors or some other unknown mechanisms might affect the transport function of NIS for astatide, explaining the difference in uptake between the stomach and the thyroid.

For K1-NIS tumor, we performed the cellular uptake analysis for the comparison of ^{211}At uptake between AA(+) ^{211}At solution and AA(-) ^{211}At solution, in which uptakes were normalized by the amount of cells. Uptake of ^{211}At was significantly increased under the AA(+) condition as compared to the

AA(-) condition in K1-NIS cells (Fig. 3B) as well as in the thyroid glands of normal rats (Fig. 2). Meanwhile, we need to consider the ethical 3R rules (replacement, reduction and refinement) in animal experiments. Therefore, we thought it is precise and ethically reasonable to compare by simultaneous cellular uptake analysis.

Petrich T et al. evaluated the treatment effect of ^{211}At in K1-NIS xenograft mice. In their study, a total activity of 2.5 MBq was intraperitoneally administered in three fractions within 16 days (*12*). Although they stated that $^{211}At^-$ was used in their experiments, there was no description of any detailed analysis of the ^{211}At solutions used in their study. In our study, we evaluated the oxidation states of ^{211}At in solution in greater detail and proved that appropriate preparation of the astatine solution using reducing agents, such as AA, is important for maximizing the treatment effect of ^{211}At in the form of astatide. They also showed that fractionated ^{211}At therapy resulted in complete remission

of the K1-NIS xenografts and also stated that single administration caused stable shrinkage for up to 8 weeks, but was followed by tumor regrowth. We observed tumor shrinkage for up to 41 days after the administration of ^{211}At (1 MBq), followed thereafter by regrowth in our study, similar to the findings of the aforementioned study. They also reported that administration of a total of 2.5 MBq of ^{211}At caused moderate damage in the thyroid by showing decreased uptake in $^{99m}TcO_4$ scintigraphy and atrophy in the histological analysis. We showed that a smaller dose (0.1 MBq) of ^{211}At is also effective for the suppression of tumor growth, although the regrowth was faster than after administration of the higher dose (0.4 MBq or 1 MBq). These results suggest that more fractionated administration can be performed during targeted alpha therapy using ^{211}At in the clinical setting to reduce the side effects in normal organs. Fractionated administration of an alpha-emitter has been successfully adapted in ^{223}Ra therapy for bone metastasis in castration-resistant prostate

cancer (*22*). Therefore, targeted alpha therapy with ^{211}At would be clinically feasible, and the short half-life of ^{211}At (7.2 hr) is more ideal for preventing potential side effects following repeated administration over a short time period.

Besides differentiated thyroid cancer, there are other cancers that show expression of NIS, such as breast cancer and gastric cancer (*23,24*). In patients with these cancers, ^{211}At therapy can be one of the treatment options, especially for those with multiple metastases, in combination with appropriate iodine blocking of the normal thyroid (*25*). Recently, other groups in Japan have successfully demonstrated the excellent treatment effect of ^{211}At-labelled antibody or compounds for the treatment of the peritoneal dissemination from gastric cancer and pheochromocytoma (*8,9*). Appropriate targeting is our next challenge, with careful evaluation of dehalogenation of the ^{211}At compounds (*13*).

In the present study, structure of the follicle was disrupted in the thyroid tissue at 3, 7 and 15 days after the administration of AA(+) ^{211}At, whereas no significant difference was observed in the structure of gastric mucosa (Supplemental fig. 1). It was suggested that ^{211}At could ablate the thyroid tissues, but no significant effect was observed in the stomach. There are some publications about the chronic toxicity of ^{211}At. L.M. Cobb, et al. reported that spleen, lymph nodes, bone marrow, gonads, thyroid glands, salivary glands and stomach were affected after administration of ^{211}At in mice (61kBq/g body weight) (*26*). However, most of them showed transient change at 14 days and returned to normal level or resulted in minimal damage at 56 days after administration, except for thyroid glands and gonads. The normal thyroid glands in the thyroid cancer patients were usually removed or ablated in the clinical settings, and it will not be a problem. For the gonads, it depends on the tolerability of the patients. Petrich et al. reported that thyroid atrophy was

observed in all mice and inflammation of the lungs and stomach/bowel were observed in some mice during 1 year follow up after total administration of 2.5 MBq of ^{211}At (*12*). It was suggested that no critical finding was observed with the administered dose below 1MBq.

This study had several limitations. First, we did not evaluate the side effects of ^{211}At, other than the thyroid and stomach. Detailed analysis of the side effects, especially in relation to the dose dependency, is the next important subject for study prior to clinical application. Second, we did not perform fractionated administration of ^{211}At in this study. This is also another important prerequisite to clinical application as well as for evaluation of the side effects. Third, we preliminary performed the *in-vitro* cellular survival assay using K1-NIS cells and confirmed dose-dependent lower cell viability in AA(+) ^{211}At compared to ^{131}I (Supplemental fig. 2). Comparison of the effectiveness of ^{211}At and ^{131}I is

essential to prove that ^{211}At therapy is more beneficial for patients who are refractory to repetitive ^{131}I treatment with preserved uptake ability of NIS.

CONCLUSION

This study revealed that increase of the radiochemical purity of astatide of ^{211}At solution by addition of ascorbic acid was associated with significantly enhanced uptake of ^{211}At by both normal thyroid tissue and differentiated thyroid cancer cells. The treatment effect of ^{211}At solution in the K1-NIS xenograft model was dose-dependent and was associated with prolonged survival, suggesting the potential applicability of targeted alpha therapy for the treatment of advanced differentiated thyroid cancer.

DISCLOSURE

This study was funded by the KAKENHI (C) (15K09955) from the Ministry of Education, Culture, Sports, Science and Technology (MEXT), and the QiSS program of the OPERA from the Japan Science and Technology Agency (JST), Japan. There is no other potential conflict of interest relevant to this article to disclose.

ACKNOWLEDGMENTS

We would like to thank Keiko Matsunaga, Takashi Kamiya, Takanori Kobayashi, and Takashi Yoshimura for their excellent technical assistance.

References

1. Maxon HR, 3rd, Englaro EE, Thomas SR, et al. Radioiodine-131 therapy for well-differentiated thyroid cancer--a quantitative radiation dosimetric approach: outcome and validation in 85 patients. *J Nucl Med.* 1992;33:1132-1136.

2. Higashi T, Kudo T, Kinuya S. Radioactive iodine (131I) therapy for differentiated thyroid cancer in Japan: current issues with historical review and future perspective. *Ann Nucl Med.* 2012;26:99-112.

3. Thies ED, Tanase K, Maeder U, et al. The number of 131I therapy courses needed to achieve complete remission is an indicator of prognosis in patients with differentiated thyroid carcinoma. *Eur J Nucl Med Mol Imaging.* 2014;41:2281-2290.

4. Schlumberger M. Target therapies for radioiodine refractory advanced thyroid tumors. *J Endocrinol Invest.* 2012;35(6 Suppl):40-44.

5. Li G, Lei J, Song L, et al. Radioiodine refractoriness score: A multivariable prediction model for postoperative radioiodine-refractory differentiated thyroid carcinomas. *Cancer Med.* 2018;7:5448-5456.

6. Haugen BR, Alexander EK, Bible KC, et al. 2015 American thyroid association management guidelines for adult patients with thyroid nodules and differentiated thyroid cancer: the American thyroid association guidelines task force on thyroid nodules and differentiated thyroid cancer. *Thyroid.* 2016;26:1-133.

7. Ogawa K, Mizuno Y, Washiyama K, et al. Preparation and evaluation of an astatine-211-labeled sigma receptor ligand for alpha radionuclide therapy. *Nucl Med Biol.* 2015;42:875-879.

8. Li HK, Morokoshi Y, Nagatsu K, Kamada T, Hasegawa S. Locoregional therapy with alpha-emitting trastuzumab against peritoneal metastasis of human

epidermal growth factor receptor 2-positive gastric cancer in mice. *Cancer Sci.* 2017;108:1648-1656.

9. Ohshima Y, Sudo H, Watanabe S, et al. Antitumor effects of radionuclide treatment using alpha-emitting meta-(211)At-astato-benzylguanidine in a PC12 pheochromocytoma model. *Eur J Nucl Med Mol Imaging.* 2018;45:999-1010.

10. Ikeda H, Hayashi Y, Takahashi N, et al. Application of astatine-210: Evaluation of astatine distribution and effect of pre-injected iodide in whole body of normal rats. *Appl Radiat Isot.* 2018;139:251-255.

11. Andersson H, Palm S, Lindegren S, et al. Comparison of the therapeutic efficacy of 211At- and 131I-labelled monoclonal antibody MOv18 in nude mice with intraperitoneal growth of human ovarian cancer. *Anticancer Res.* 2001;21:409-412.

12. Petrich T, Quintanilla-Martinez L, Korkmaz Z, et al. Effective cancer therapy with the alpha-particle emitter [211At]astatine in a mouse model of genetically

modified sodium/iodide symporter-expressing tumors. *Clin Cancer Res.* 2006;12:1342-1348.

13. Teze D, Sergentu DC, Kalichuk V, et al. Targeted radionuclide therapy with astatine-211: Oxidative dehalogenation of astatobenzoate conjugates. *Sci Rep.* 2017;7:2579.

14. Appelman EH. The oxidation states of astatine in aqueous solution. *J Am Chem Soc*. 1961;83:805–807.

15. Kurosawa H, Sakurai K, Hasegawa H, et al. Comparison of radioactive iodide uptake in the rat thyroid between oral and intravenous bolus administration. *Ann Nucl Med.* 2014;28:986-993.

16. Kuikka JT, Yang J, Kiiliainen H. Physical performance of the Siemens E.CAM gamma camera. *Nucl Med Commun.* 1998;19:457-462.

17. Johnson EL, Turkington TG, Jaszczak RJ, et al. Quantitation of 211At in small volumes for evaluation of targeted radiotherapy in animal models. *Nucl Med Biol.* 1995;22:45-54.

18. Spetz J, Rudqvist N, Forssell-Aronsson E. Biodistribution and dosimetry of free 211At, 125I- and 131I- in rats. *Cancer Biother Radiopharm.* 2013;28:657-664.

19. Carlin S, Mairs RJ, Welsh P, Zalutsky MR. Sodium-iodide symporter (NIS)-mediated accumulation of [(211)At]astatide in NIS-transfected human cancer cells. *Nucl Med Biol.* 2002;29:729-739.

20. Visser GWM, Diemer EL. Inorganic astatine chemistry. *Radiochim Acta.* 1983;33:145-51.

21. Darrouzet E, Lindenthal S, Marcellin D, Pellequer JL, Pourcher T. The sodium/iodide symporter: state of the art of its molecular characterization. *Biochim Biophys Acta.* 2014;1838:244-253.

22. Saad F, Carles J, Gillessen S, et al. Radium-223 and concomitant therapies in patients with metastatic castration-resistant prostate cancer: an international, early access, open-label, single-arm phase 3b trial. *Lancet Oncol.* 2016;17:1306-1316.

23. Yao C, Pan Y, Li Y, et al. Effect of sodium/iodide symporter (NIS)-mediated radioiodine therapy on estrogen receptor-negative breast cancer. *Oncol Rep.* 2015;34:59-66.

24. Shiozaki A, Ariyoshi Y, Iitaka D, et al. Functional analysis and clinical significance of sodium iodide symporter expression in gastric cancer. *Gastric Cancer.* September 6, 2018. [Epub ahead of print]

25. Joseph JK, Patel RB, Damle AA, Nair N, Badwe RA, Basu S. Functional radionuclide imaging, in-vitro radioiodine uptake estimation and RT-PCR in the evaluation of sodium iodide symporter (NIS) expression and functionality in breast cancer: a pilot study. *Indian J Surg Oncol.* 2013;4:80-91.

26. Cobb LM, Harrison A, Butler SA. Toxicity of astatine-211 in the mouse. *Hum Toxicol.* 1988;7:529-534.

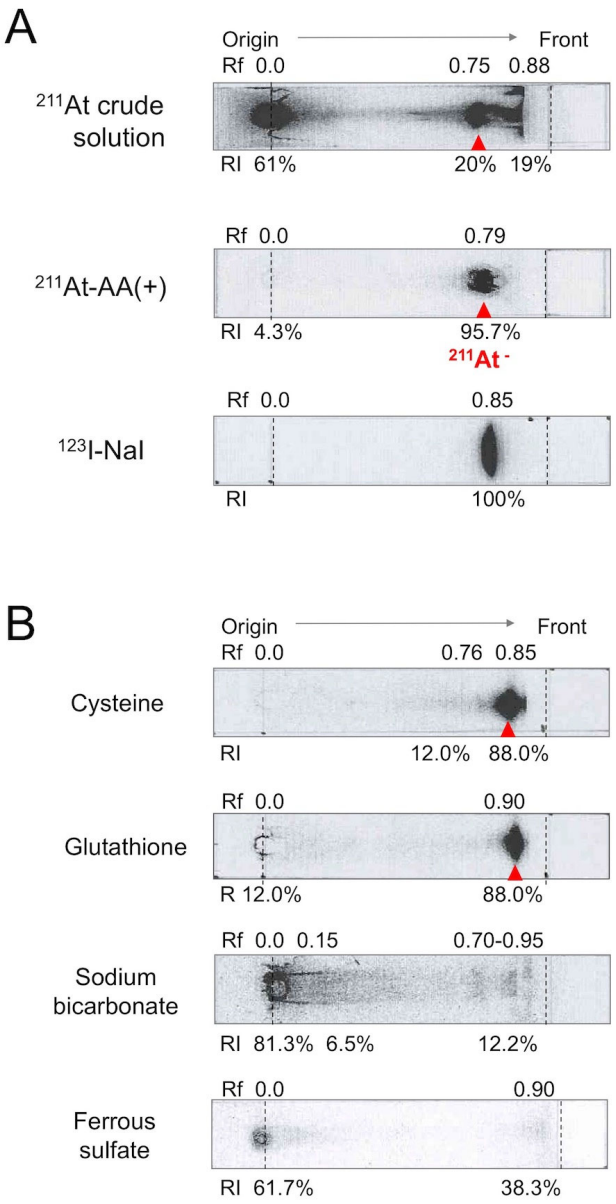

FIGURE 1. (A) TLC profiles of the ^{211}At solutions and a^{123}I-NaI solution. (B) TLC profiles of the ^{211}At solutions after addition of various reducing agents (1 w/v%).

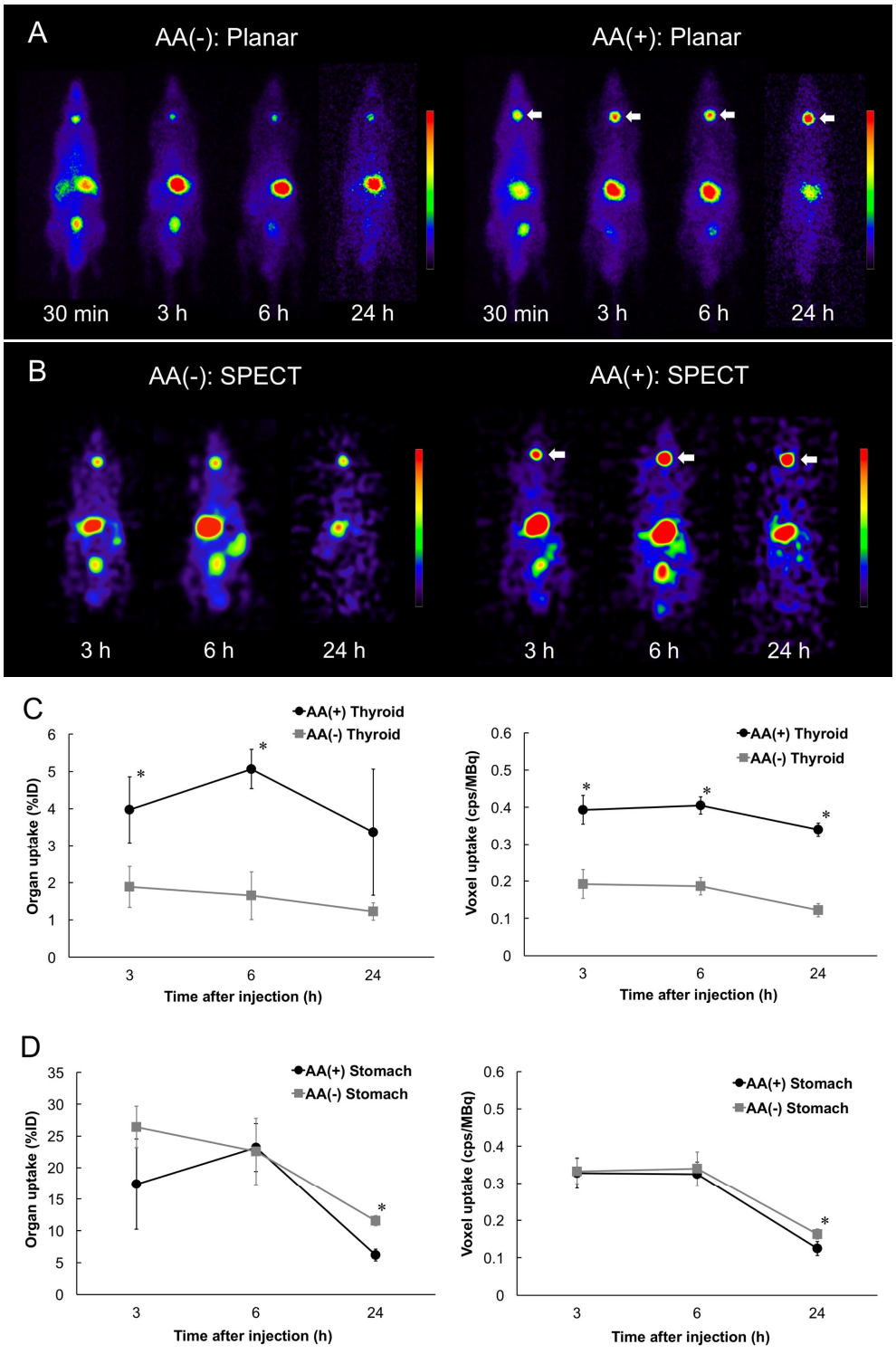
A
AA(-): Planar
AA(+): Planar
30 min
3 h
6 h
24 h
30 min
3 h
6 h
24 h
B
AA(-): SPECT
AA(+): SPECT
3 h
6 h
24 h
3 h
6 h
24 h
C
AA(+) Thyroid
AA(-) Thyroid
Organ uptake (%ID)
Time after injection (h)
AA(+) Thyroid
AA(-) Thyroid
Voxel uptake (cps/MBq)
Time after injection (h)
D
AA(+) Stomach
AA(-) Stomach
Organ uptake (%ID)
Time after injection (h)
AA(+) Stomach
AA(-) Stomach
Voxel uptake (cps/MBq)
Time after injection (h)

FIGURE 2. (A) Planar and (B) SPECT images of normal rats: AA(-) group (crude ^{211}At solution) and AA(+) group (^{211}At solution treated with ascorbic acid). Increased uptake was observed in the thyroid gland (arrows) under the AA(+) condition as compared to the AA(-) condition. (C,D) Time-activity curves in the thyroid and stomach after injection of ^{211}At solution on planar (%ID) and SPECT (cps/MBq) images (*: $p < 0.05$).

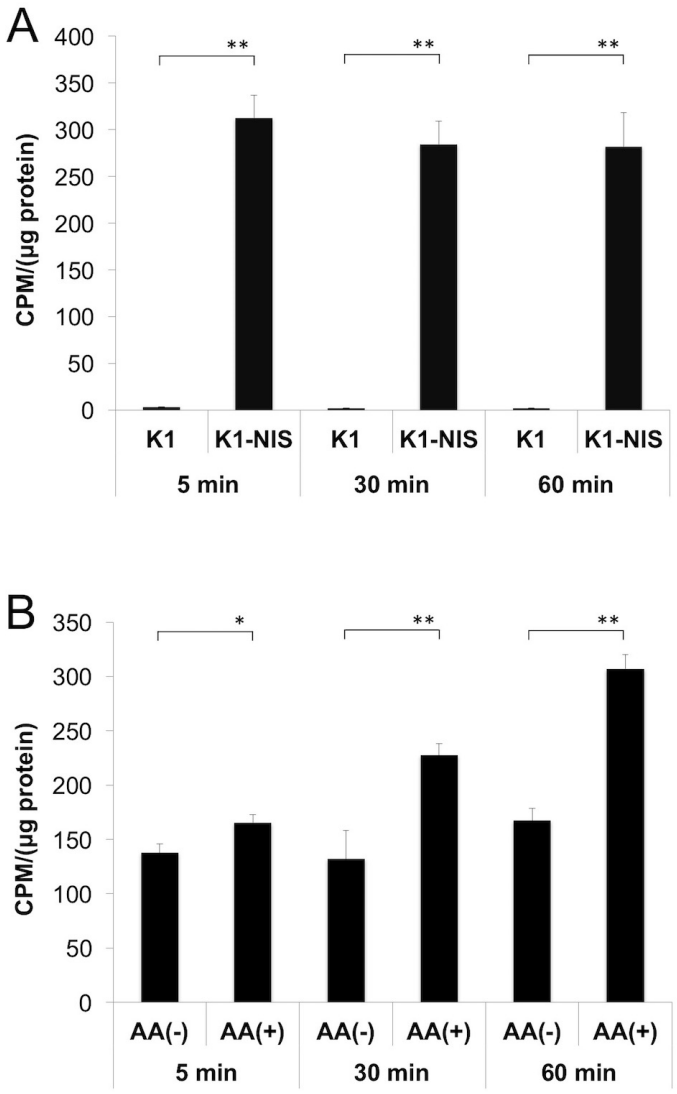

FIGURE 3. (A) In-vitro uptake analysis of ^{211}At uptake in the K1 and K1-NIS cells, (B) comparison of ^{211}At uptake in the K1-NIS cells between AA(-) and AA(+) solutions. (*: $p < 0.05$ and **: $p < 0.01$).

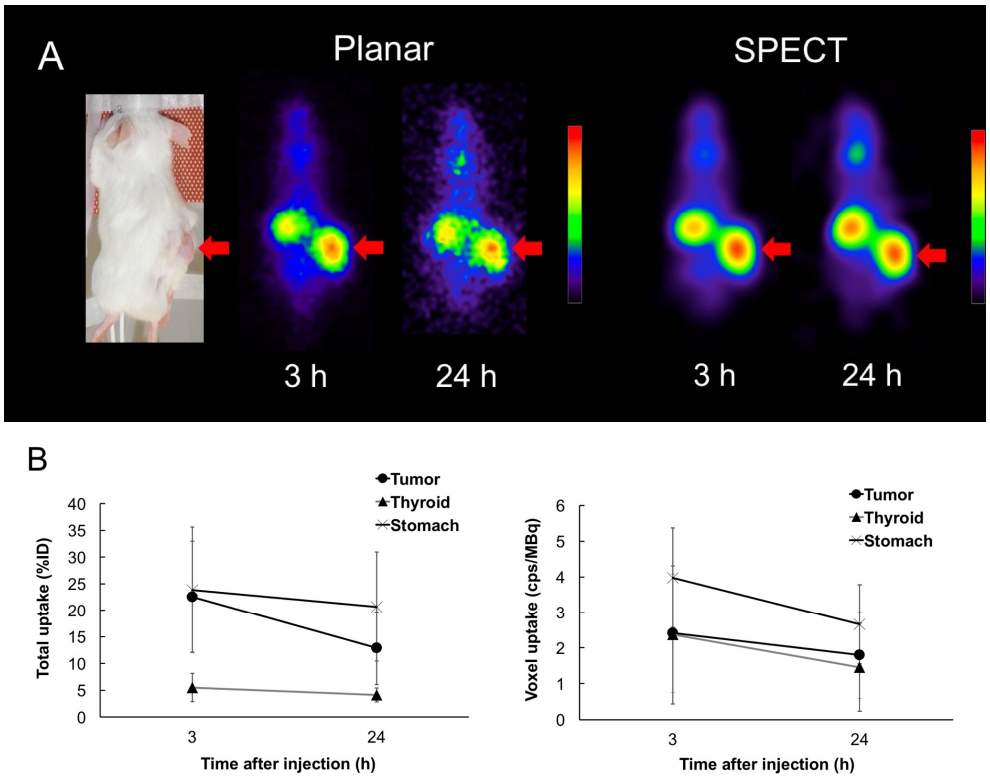

FIGURE 4. (A) Planar and SPECT images of the mouse K1-NIS xenograft model after injection of AA(+) solution. High uptake was observed in the xenografts (arrows). (B) Uptakes of ^{211}At in the tumor xenograft, thyroid, and stomach at 3 hr and 24 hr post injection of AA(+) solution.

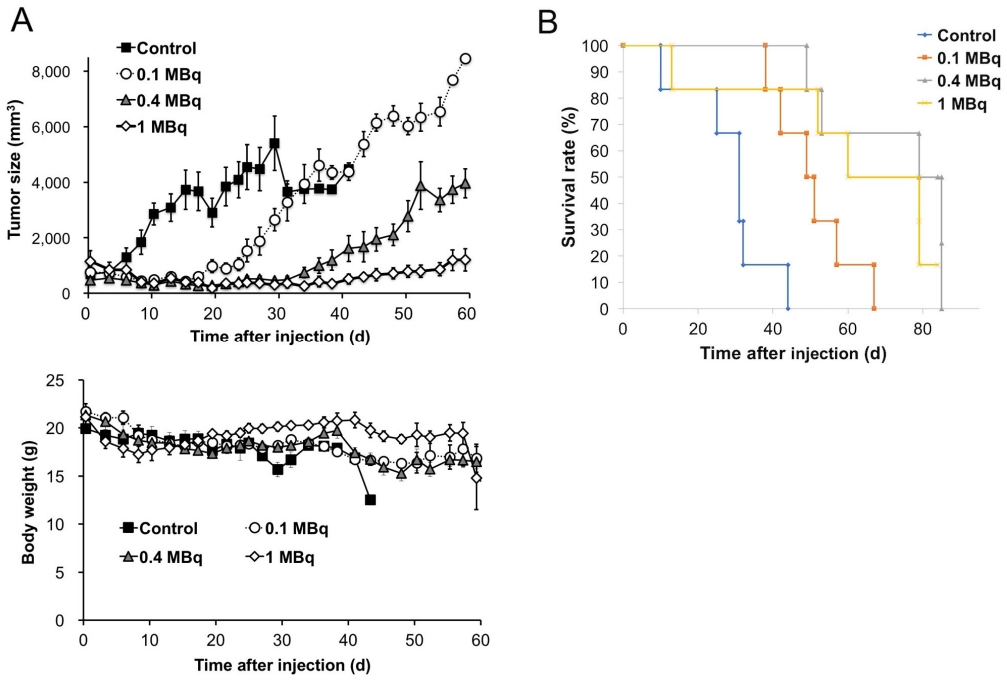

FIGURE 5. Treatment response after administration of AA(+) solutions. (A) Change in the tumor size and body weight after administration of AA(+) solutions. (B) Kaplan Meier analysis for comparison of survivals.

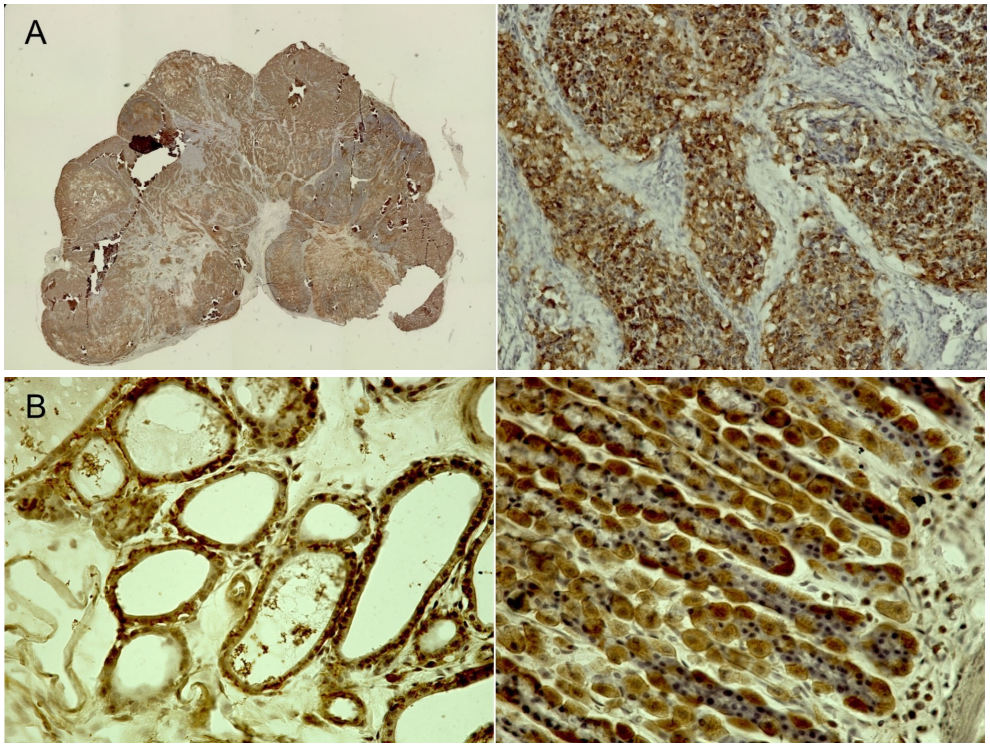

FIGURE 6. Immunohistochemical staining for NIS (anti-SLC5A5 rabbit IgG): (A) K1-NIS xenograft at low magnification (left), K1-NIS xenograft at high magnification (right), (B) thyroid (left) and stomach wall (right) of a normal rat. Cells showing NIS expression are stained brown.

	AA(-)	AA(+)	
	Mean ± SE (%ID/g)	Mean ± SE (%ID/g)	p-value
Brain	0.03 ± 0.02	0.02 ± 0.00	0.89
Thyroid	61.7 ± 16.2	417.6 ± 108.3	0.03*
Submandibular gland	0.20 ± 0.01	0.17 ± 0.02	0.44
Heart	0.24 ± 0.02	0.24 ± 0.03	0.25
Lung	0.78 ± 0.18	0.84 ± 0.05	0.28
Thymus	0.20 ± 0.02	0.35 ± 0.06	0.02*
Liver	0.21 ± 0.07	0.11 ± 0.00	0.75
Stomach	3.36 ± 1.16	3.56 ± 0.15	0.18
Small intestine	0.31 ± 0.06	0.30 ± 0.02	0.25
Large intestine	0.29 ± 0.01	0.56 ± 0.13	0.15
Cecum	0.36 ± 0.05	0.41 ± 0.08	0.14
Kidney	0.33 ± 0.03	0.29 ± 0.02	0.40
Adrenal gland	0.19 ± 0.04	0.13 ± 0.01	0.45
Pancreas	0.15 ± 0.01	0.13 ± 0.05	0.55
Spleen	1.13 ± 0.22	1.36 ± 0.28	0.14
Testis	0.35 ± 0.01	0.35 ± 0.02	0.25
Blood	0.12 ± 0.02	0.13 ± 0.00	0.24

TABLE 1. Comparison of whole-body distribution after intravenous administration of ^{211}At solutions between AA(-) group (crude ^{211}At solution) and AA(+) group (^{211}At solution treated with ascorbic acid). Data are expressed as the mean values with standard error (SE).

	Mean ± SE (%ID/g)
Thyroid	101.9 ± 27.0
Salivary gland	10.4 ± 6.1
Liver	2.8 ± 0.8
Stomach	22.1 ± 10.9
Kidney	3.6 ± 0.7
Pancreas	2.6 ± 0.4
Spleen	4.6 ± 1.6
Testis	2.7 ± 0.1
Lung	10.6 ± 3.5
Small intestine	2.5 ± 0.3
Tumor	8.3 ± 3.1

TABLE 2. Whole-body distribution after intravenous administration of AA(+) solution in the mouse K1-NIS xenograft model (n = 3). Data are expressed as the mean values with standard error (SE).

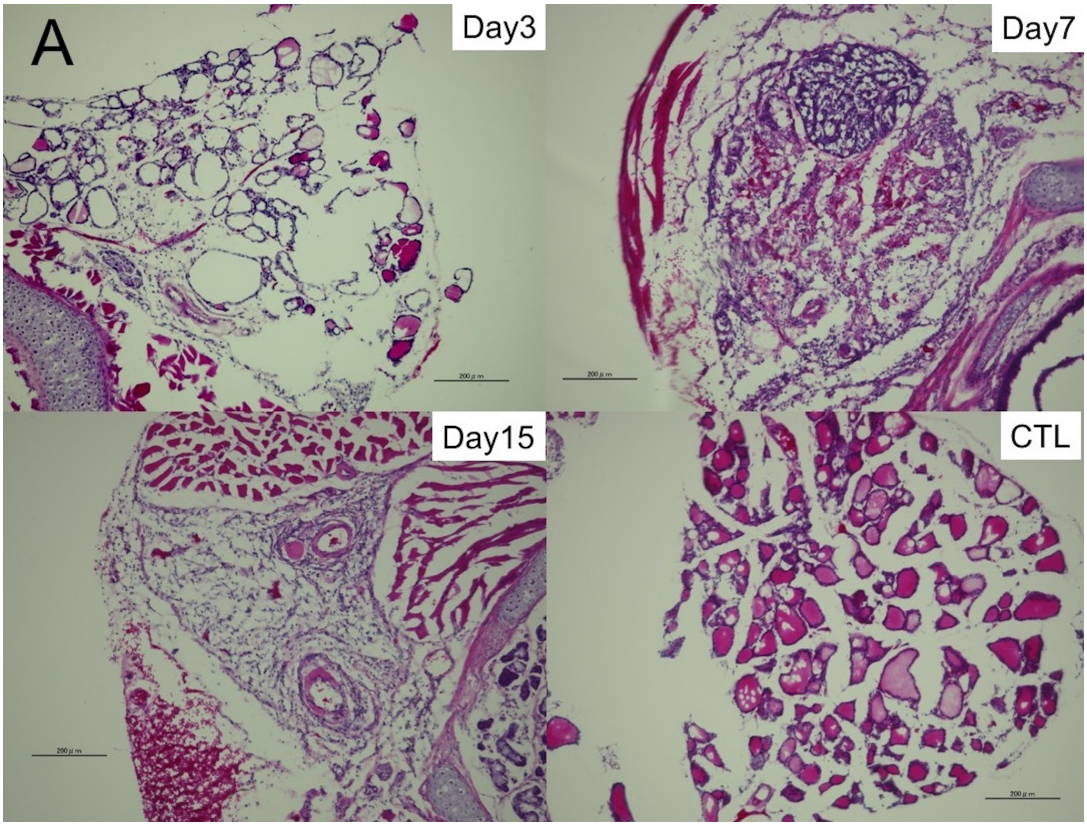
A
Day3
Day7
Day15
CTL

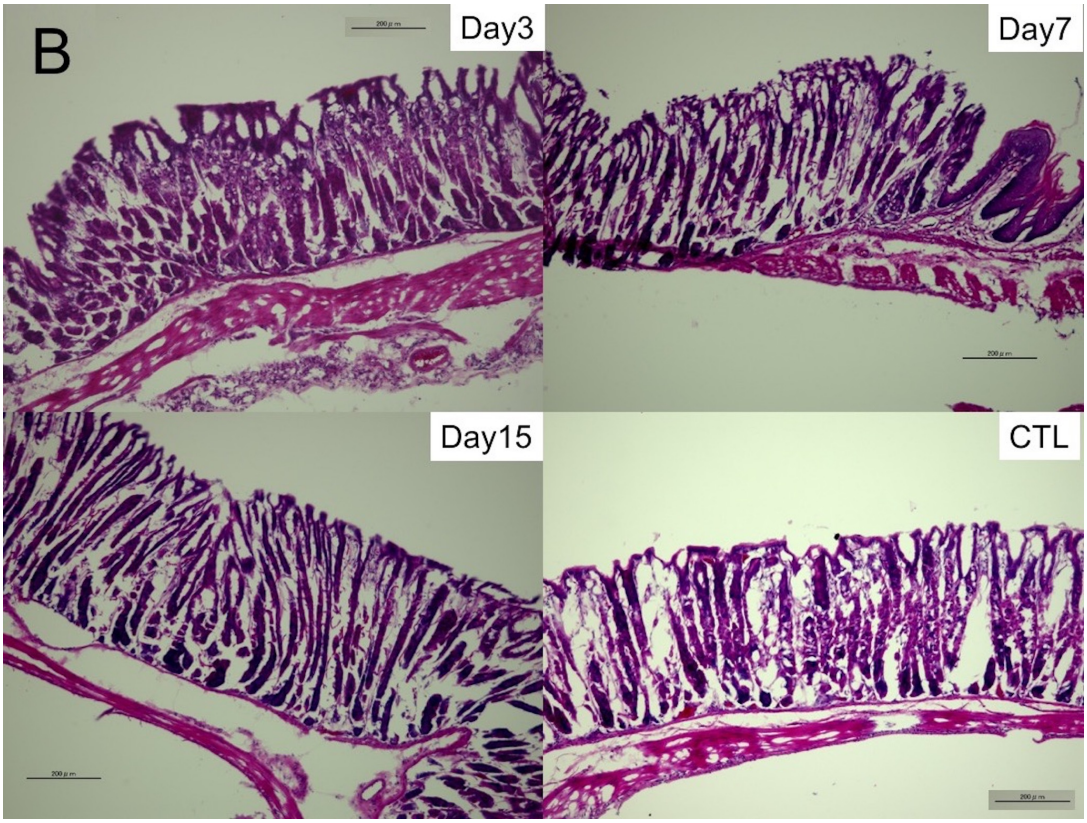

Supplemental figure 1. H&E staining of the (A) thyroid gland and (B) stomach in normal ICR mice at 3, 7 and 15 days after administration of AA(+) ^{211}At solution (1 MBq) and control (CTL). Bar indicates 200μm.

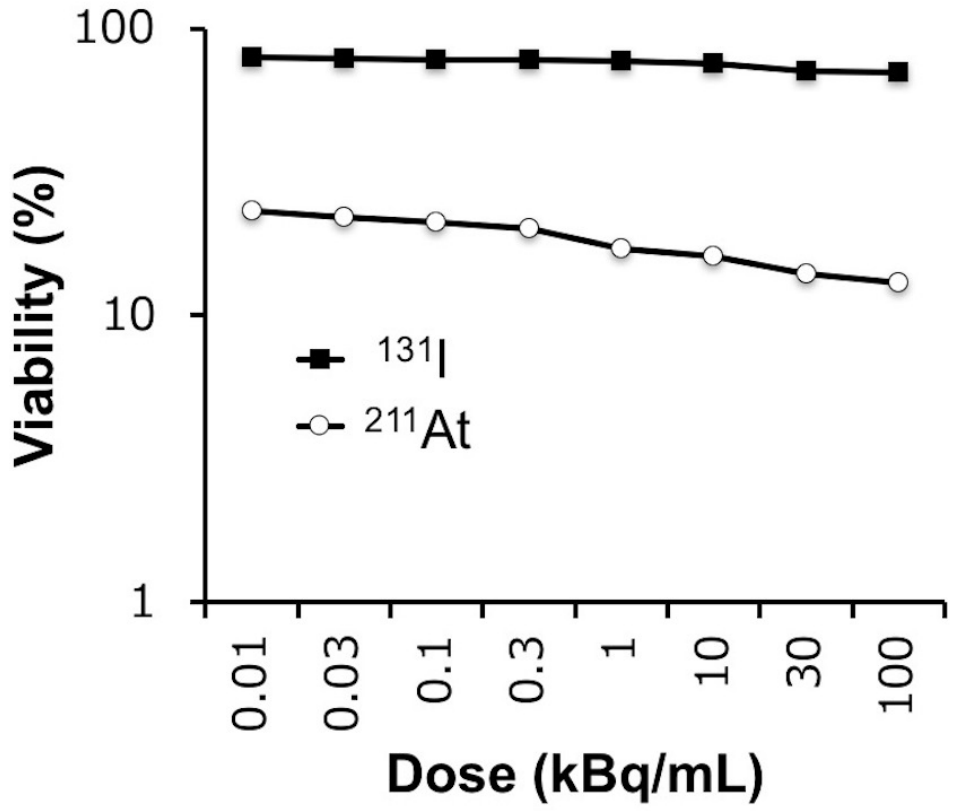

Supplemental figure 2. *In-vitro* cellular survival assay using K1-NIS cells for the comparison between ^{131}I and AA(+) ^{211}At.